ISSN 1061-8309, Russian Journal of Nondestructive Testing, 2024, Vol. 60, No. 5, pp. 481–500. © Pleiades Publishing, Ltd., 2024.
Russian Text © The Author(s), 2024, published in Defektoskopiya, 2024, No. 5, pp. 13–35.

ACOUSTIC METHODS

Modeling Defects in Ultrasonic Nondestructive Testing: State-of-the-Art and Prospects

L. Yu. Mogilner[a,b,*], V. A. Syasko[c,], and A. I. Shikhov[d,***]**

[a] *Bauman Moscow State Technical University, Moscow, 105005 Russia*
[b] *Welding and Control Scientific and Training Center, Bauman Moscow State Technical University, Moscow, 105005 Russia*
[c] *Konstanta Ltd., St. Petersburg, 199106 Russia*
[d] *St. Petersburg Mining University, St. Petersburg, 199106 Russia*
**e-mail: mogilner@mail.ru*
***e-mail: 9334343@gmail.com*
****e-mail: shihov-gol@mail.ru*

Received April 17, 2024; revised May 3, 2024; accepted May 3, 2024

Abstract—In the introduction to the article we mention four factors that are most important for ensuring the accuracy of characterizing defects during ultrasonic inspection, viz., parameters of artificial reflectors in samples, compliance of the acoustic properties of the material of tuning samples and tested products, transient characteristics of electroacoustic paths, and methodological features of measurements. The present article is devoted to the analysis of the first and partly fourth of listed factors. The review of reflectors, the use of which is regulated in various standards, is carried out. Advantages and disadvantages of flat-bottomed holes, segmental and corner reflectors ("notches"), lateral (SDH) and vertical cylindrical holes, and grooves are noted. Taking into account the specific features of ultrasonic wave scattering, it is noted that artificial "reflectors" such as "grooves" and SDHs are used to adjust the parameters of modern diffraction testing methods. It is recommended to expand the use of grooves, SDHs, and vertical drilling when revising the standards governing the use of conventional echo methods. The estimation of accuracy of measurement of defects parameters, first of all, the crack tip coordinates, with application of modern digital methods of information processing during ultrasonic testing is given. It is indicated that to increase the measurement accuracy and to determine the position and orientation of cracks in welds, it is necessary to create a database of digital twins of samples with artificial reflectors and products with real defects. A general scheme of executing the quality control is given that takes into account the use of standards (measures), digital models of artificial reflectors, and digital twins of the testing process to ensure the necessary detectability of defects and reliability of manual, automated, and, potentially, automatic testing.

Keywords: ultrasonic testing, metrological support, defect modelling, artificial reflector, dimensional measurement, digital twin

DOI: 10.1134/S1061830924700657

INTRODUCTION

At the end of the 20th century, the technology of ultrasonic echo method monitoring reached a certain saturation: small-sized electronic equipment was used and maximum information was extracted from A-scans on the display of flaw detectors, i.e., from the representation of signals due to defects in time–amplitude coordinates. Diffraction methods have also been used, but mainly as an aid to clarify the results [1–3]. At the same time, "standard" and tuning samples with prepared artificial defects with specified dimensions were used to set up and check the equipment.

Since the beginning of this century, the technique and technology of flaw detection, including ultrasonic quality control, has moved to a new stage of development. Modern digital equipment equally uses echo and diffraction ultrasonic testing methods. This makes it possible to obtain acoustic images (tomograms) of various sections of tested products and welds of various configurations and sew them into three-dimensional images (see, for example, [4–7]). When solving theoretical and applied problems, nondestructive testing moves from flaw detection, i.e., the ability to detect a defect, to flaw sizing, i.e., to measuring the defect parameters in a product. The task is to perform measurements with the accuracy

necessary for calculating the operational characteristics and resource of the examined object [8–12]. At the same time, approaches to setting up and checking equipment require adjustments, and questions about the error in measuring the defect sizes and determining their type and orientation come to the fore, including during automated and automatic testing of products during their manufacture and installation, as well as during periodic diagnostics in operation. When developing new approaches, it is advisable to make greater use of the experience gained in related industries such as biotechnologies, medicine, geophysics (see, for example, [13–16]).

Based on the above, it seems relevant to consider the factors that are most important for ensuring the accuracy of measurements during ultrasound testing. First of all, it is necessary to take into account the shape, size, and orientation of artificial reflectors in the samples [1, 2, 17–19], the relation between acoustic properties of tuning samples and real products [20–22], the transient characteristics of electroacoustic paths of ultrasonic transducers [1, 2, 23, 24], and methodological features of taking measurements [3, 24, 25].

In this paper, we consider the first of these factors, including the sample stock and the current requirements for artificial reflectors that are used to set up and test equipment for pulsed ultrasonic testing, and outline the directions of development in this area. At the same time, we emphasize some of the features that seem to remain most relevant at the present time. Also, taking into account the established practice of using digital data processing methods, we consider some areas of improvement of techniques and technology for characterizing defects using reflectors of various types.

BOTTOM SURFACE

Let us briefly outline the issue of setting up the depth gauge of a pulse ultrasonic flaw detector or the thickness gauge. It is well known that this operation is based on measuring the reception time of the ultrasonic pulse reflected from the bottom surface of the sample [1, 26]. For example, a 3 mm thick plate fixed to the device body or a set of steps with a thickness in a given range can be used. In domestic practice, the verification of thickness gauges was carried out using a set of measures KUSOT-180; this set is plane-parallel and the measures in it possess different surface roughness and curvature. Analogs are also being produced at the present time (see, for example, the website [27]).

The basic operations required to set up and verify the thickness gauge are extremely simple (Fig. 1) and can be performed on longitudinal (for piezoelectric transducers—PETs) or transverse waves (for electromagnetic acoustic transducers—EMATs). The time t of receiving the bottom signal is measured (if required, minus the ultrasonic wave delay time t_1 in the PET wedge or taking into account a series of bottom reflections), and the depth gauge readings are calibrated according to the thickness value determined by the formula

$$S = \frac{1}{2}v(t - t_1), \tag{1}$$

where S is the "measured" thickness of the sample, and v is the velocity of ultrasonic (longitudinal or transverse) waves. The measurement error is determined by the relation

$$\Delta S = \frac{1}{2}\left\{\frac{2S}{v}\Delta v + v(\Delta t + \Delta t_1)\right\}, \quad \frac{\Delta S}{S} = \left\{\frac{\Delta v}{v} + \frac{\Delta t + \Delta t_1}{t - t_1}\right\}, \tag{2}$$

where Δ is the measurement (or setting) error of the corresponding quantities.

Usually, the instrument absolute permissible error of thickness gauging is set in the passport of the ultrasonic thickness gauge in the form $(A + 0.01X)$, where A is the random component of the error, and X is the nominal value of the measured thickness. For example, for $A = 0.1$ mm and $X = 10$ mm, the relative error $\Delta S/S$ is 2%. However, it should be borne in mind that according to [20–22], in formula (2) the difference in the velocity of ultrasonic waves in the tested material and in the tuning sample can be 10% or more. As a result, the thickness measurement error may substantially exceed the data provided in the thickness gauge data sheets [28].

Bearing in mind the prospect of developing the ultrasonic thickness gauging, we note some new opportunities provided by the use of cross-section images of the product on the digital device display. In Fig. 2a, the reception time of bottom signals can be recorded both based on the A-scan (yellow scan line at the display bottom) and B-scan (cross-section image). In Fig. 2b, when sounding coarse-grained material, the bottom signals on the A-scan are practically indistinguishable, but the bottom surface is visible on the B-scan. According to [28], in this example, the thickness of the material was 26 ± 2 mm, i.e., the mea-

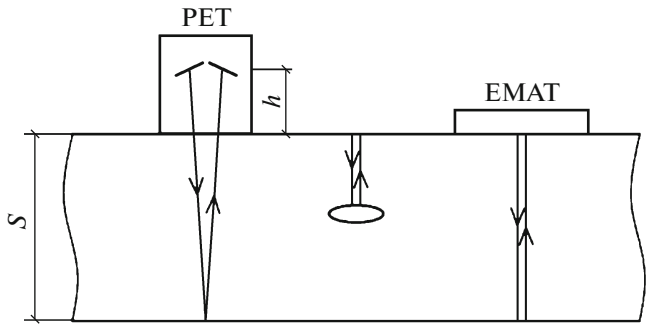

Fig. 1. Scheme of setting the depth gauge and measuring material thickness.

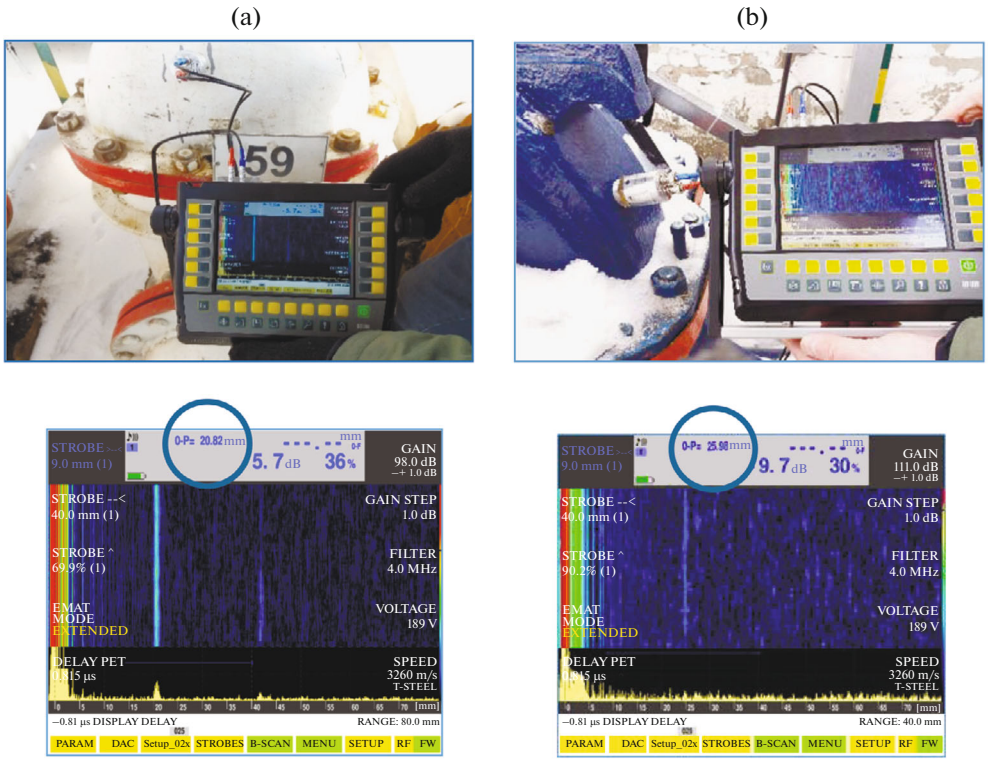

Fig. 2. Measuring cast material thickness over a rough surface with relatively small (a) and large (b) attenuation coefficient of ultrasonic waves [11, 28].

surement error was approximately 8%. Obviously, due to the pulse broadening and its less clear boundaries, there is no need to mention precise measurements here. However, the result may be sufficient to assess the technical condition of products made of coarse-grained materials with nonparallel rough surfaces (cast valve housings, pumps, etc.). In the presence of stratification, its occurrence depth can also be determined with an error sufficient to perform strength verification calculations.

CALIBRATION BLOCKS, MEASURES AND TUNING SAMPLES WITH ARTIFICIAL DEFECTS

Let us consider other reflectors using the example of the “SO-1 calibration block” according to [29] and previous versions of this standard published before 1972. This sample is not included in the current standard [17]. However, throughout the ultrasonic testing evolvement, its use was mandatory in the practice of ultrasound testing.

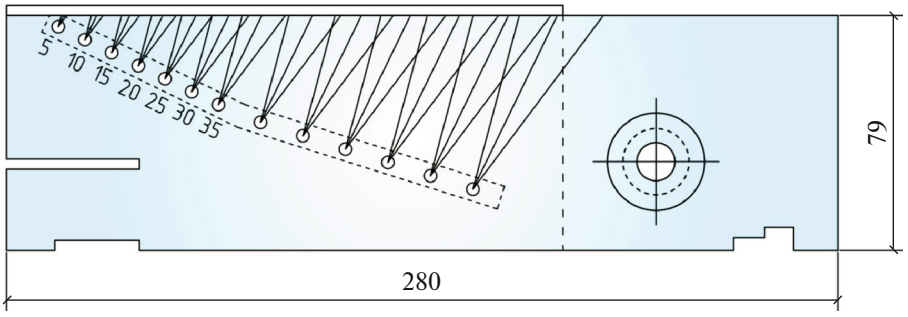

Fig. 3. SO-1 Plexiglass® calibration blocks.

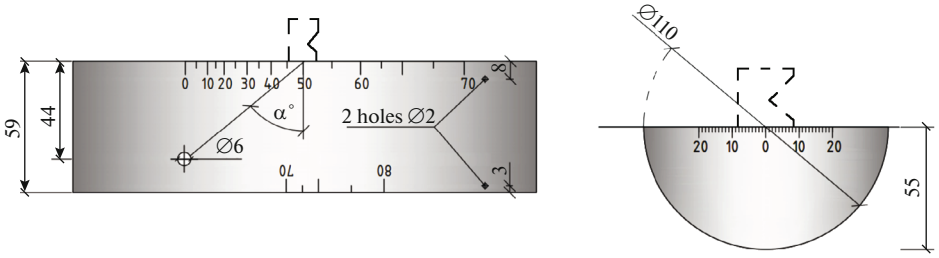

Fig. 4. SO-2 and SO-3 steel calibration blocks.

The SO-1 block was made of Plexiglass® (polymethylmethacrylate) (Fig. 3). The "conditional" sensitivity of a PET–flaw-detector pair was measured using SDHs with a diameter of 2 mm. The "conditional" sensitivity was the name chosen for the maximum depth of location of an SDH (in millimeters) that can be detected with the selected equipment parameters. Also, the SO-1 block was used to check and adjust the depth gauge based on the signal due to a horizontal cut. Finally, using the SO-1 block, it was possible to estimate the ray resolution of the PET–flaw-detector pair. For this purpose, grooves and bottom surface were used for a straight beam PET and cylindrical drilling of various diameters, for angle PETs. Note that the current standard [17] does not provide for a mandatory resolution check. It should also be noted that the SO-1 block was primarily intended for working with wedges (PETs) made of Plexiglass®, while in recent years materials with other acoustic properties have often been used to manufacture wedges.

In the current documents, the term "calibration block" has been replaced by the term "measure" [17, 30]. This is the name for products of special shapes and sizes in the material of which "artificial defects," or, as indicated above, "reflectors" have been prepared.

According to [17], SO-2 and SO-3 blocks (Fig. 4) and their variant SO-3R with reflectors are used to check and configure the equipment:

– The flat surfaces of SO-2 and SO-3 are used for depth gauge calibration.

– The cylindrical surface of SO-3 is used for determining the position of the ultrasonic beam entry point.

– The SDH with a diameter of 2 mm in SO-2 is used for checking the dead zone of the "ultrasonic-transducer–flaw-detector" pair.

– The SDH with a diameter of 6 mm in SO-2 is used to determine the angle of entry of ultrasonic waves into steel and adjust the sensitivity of the ultrasonic-transducer–flaw-detector pair.

It is also allowed to use samples V1 and V2 (Fig. 5), adopted in foreign practice [3, 18, 19]. The diameters of these SDHs in the samples are 1.5 and 5 mm, respectively, i.e., they differ from the SDH in SO-2. The groove in the V1 sample, together with the adjacent flat surfaces, is used to check the ray resolution of the ultrasonic-transducer–flaw-detector pair.

Note. When checking the parameters of ultrasonic testing by measures and other samples, the above-mentioned remarks about the speed of ultrasonic waves should be borne in mind.

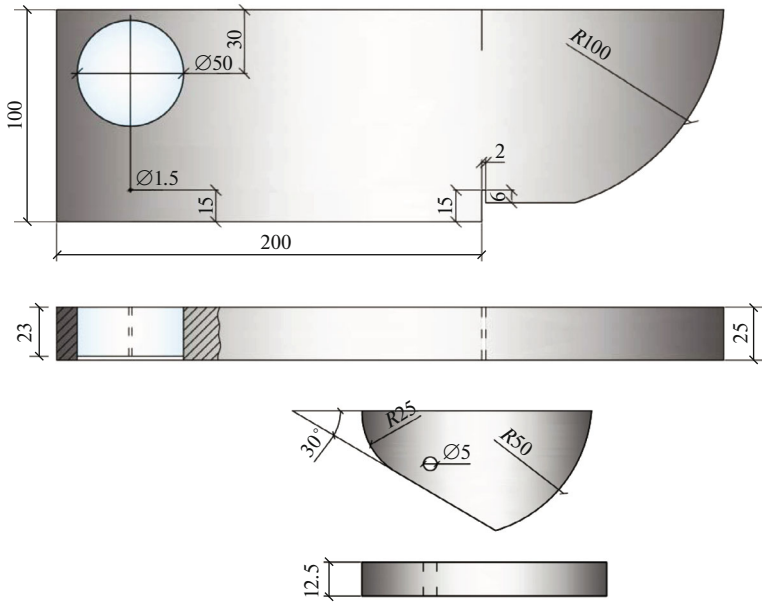

Fig. 5. V1 and V2 steel calibration blocks.

We will return to the important issue of the "groove"-type reflector below, and here we will consider other "reflectors" in "tuning" samples used when performing ultrasonic testing. Following the work by Prof. I.N. Ermolov, it is necessary to start with a cylindrical hole with flat bottom (a flat-bottomed artificial reflector), Fig. 6a [24, 31]. Based on the geometric acoustics approximation, in the works listed above as well as foreign publications, for example, [3], it is shown that the amplitude A_n of an echo signal specularly reflected from epy flat bottom drilling is related to the radius b_F of this drilling (or the area of its bottom S_F), the distance to the reflector r, and the wavelength λ by the relation [24]

$$A_i \sim \frac{S_i}{\lambda^2 r^2} = \frac{\pi b_F^2}{\lambda^2 r^2}. \quad (3)$$

On this basis, DGS diagrams i.e., nomograms have been developed that allow estimating the "equivalent" area (or diameter) of a defect by the amplitude and the time of receiving the echo signal due to the defect as the area (or diameter) of flat bottom drilling the amplitude of the reflected echo signal from which is equal to the amplitude of the echo signal received from the defect. An example of such a nomogram is shown in Fig. 7.

Flat bottom drilling has been widely used, including in domestic practice. However, the difficulties associated with its application are well known. First, in order to consider a reflection specular, it is necessary that the drilling diameter be sufficiently large compared to the wavelength of the ultrasonic wave. At conventional frequencies of 0.6–5 MHz, the minimum transverse wavelength in steel is 0.62 mm. Hence, there are restrictions on the use of DGS diagrams to estimate the equivalent area of small defects (with a diameter of approximately less than 2–3 mm) when checking products and welded joints of small thicknesses (approximately 20 mm or less). In addition, it is obviously quite difficult to check the flatness and roughness, as well as calibrate the bottom of a small diameter drill. Therefore, often, especially when setting up equipment for monitoring products (a wall) of small thickness, other reflectors are used, for example, segmental (Fig. 6b) and corner ("notch," Fig. 6c) reflectors, which simulate defects that come to the surface of welds—lack of weld penetration, undercuts, and lack of fusion along the edge.

According to [11, 17, 31], it is assumed that the amplitudes of signals specularly reflected by a drilling with a flat bottom A_n and by a segmental reflector A_{seg} are equal if they are equally oriented, are located at the same depth, and have the same area $S_F = S_{seg}$. In this case, A_n is calculated using (3). Obviously, the dimensions of the segmental reflector should be such that it is possible to talk about the specular reflection of ultrasonic waves from its inclined surface. According to [30], this requires the following conditions: $h > \lambda$ and $h/b > 0.4$, where b is the length of the intersection line between the inclined segment and the sample surface.

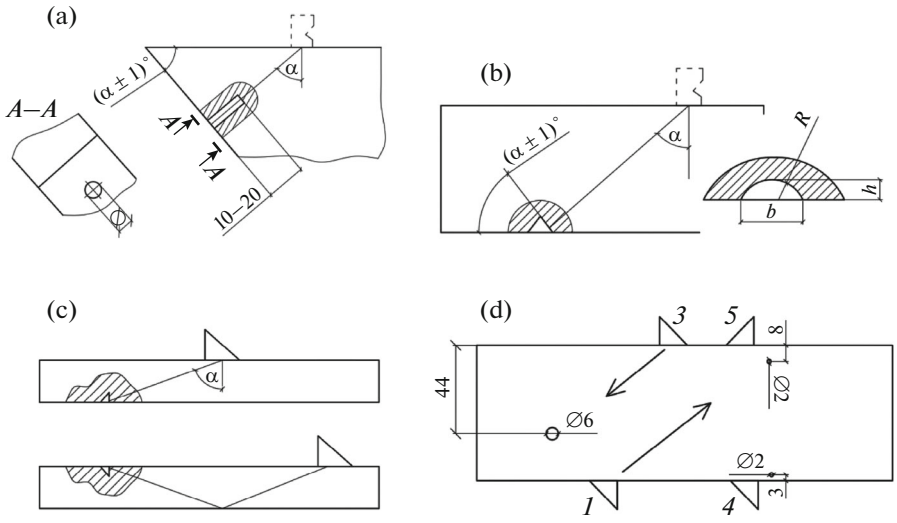

Fig. 6. Reflectors in tuning samples: (a) flat-bottom drilling, (b) segmental reflector, (c) corner reflector, (d) SDH.

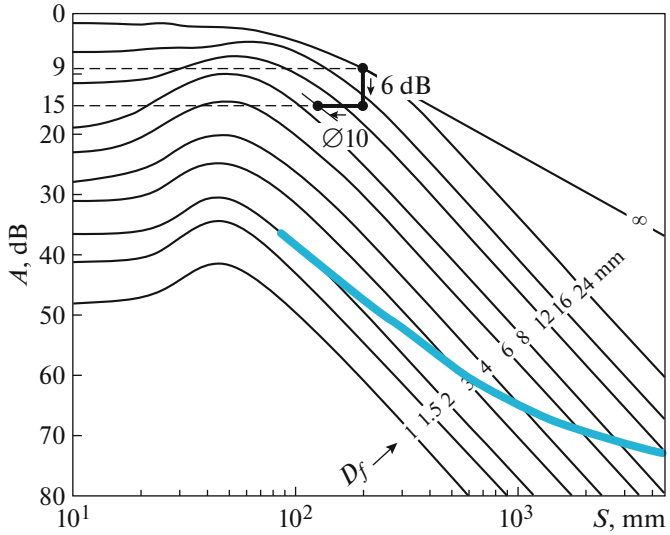

Fig. 7. Example of I.N. Ermolov DGS diagram. The black curves stand for a flat-bottomed drilling. For comparison, the blue curve is for an SDH.

The requirements for the size and orientation of the corner reflector can also be found in [29]: $b, h > \lambda$ and $h/b = 0.5–4$. Recalculation of the area $S_y = hb$ of the vertical face of the notch into the flat-bottomed drilling area is performed according to the formula

$$S_F = NS_y, \tag{4}$$

where the coefficient N is determined by the angle of ultrasonic wave entry according to the graph in Fig. 8. However, the problem is that the requirements for the size and orientation of segmental and, in particular, corner reflectors are also very difficult to fulfill.

For clarification, it is advisable to provide a reference on the notch history. The curve shown in Fig. 8 was published in the journal *Defektoskopiya* in 1973, i.e., more than 50 years ago [32]. An explanation of the nature of this curve was published 6 years later in the papers [33], in which it was found that the signal scattered by a notch is formed as a result of interference of several components. When a transverse wave is incident on the bottom surface of the sample at the third critical angle, the main contribution is made by a specular reflection by the notch (calculated by the virtual source method) and a lateral (or head)

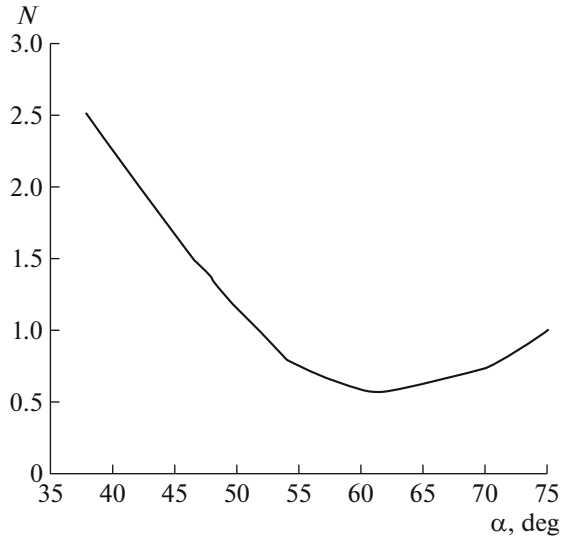

Fig. 8. Correction to the maximum sensitivity when using a notch [17].

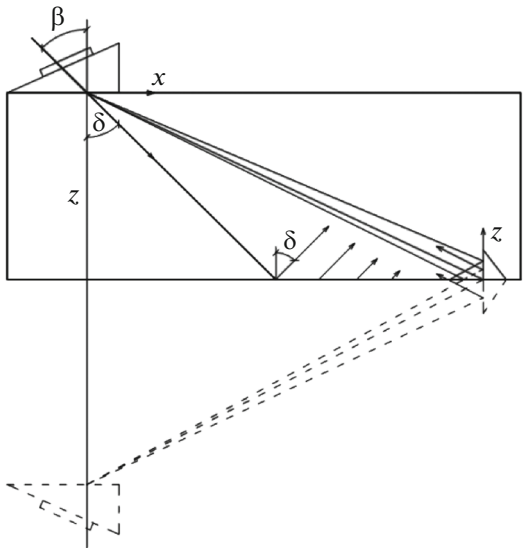

Fig. 9. Scheme for calculating echo signal due to a notch [33].

wave, excited on the bottom surface and reflected from the vertical face of the notch (Fig. 9). If a transverse wave is incident at the third critical angle on the vertical face of the notch, then it is the lateral wave occurring on this face that contributes to the resulting signal. Signals diffracted by the notch edges are also formed. The result of interference of these signals depends on the size and orientation of the notch, as well as on the angle of entry of ultrasonic waves, which explains the type of dependence in Fig. 8. The situation is similar for a segmental reflector. Currently, the influence of diffraction effects on the formation of the resulting signals seems obvious. However, in the 1970s, the study of these effects was just beginning.

The riveting, which is formed on the metal surface during the manufacture of a notch by hitting with a specially shaped striker or pressing with a solid-state indenter (see, for example, [34]), changes the acoustic properties of the material. It is also difficult to meet the requirements for the dimensions, orientation, and roughness of the vertical face. In some sources, it is proposed to make a notch on precision machines under factory conditions. However, as mentioned above, the acoustic characteristics of the samples, including the ultrasonic wave velocity, almost always differ from the characteristics of the tested material.

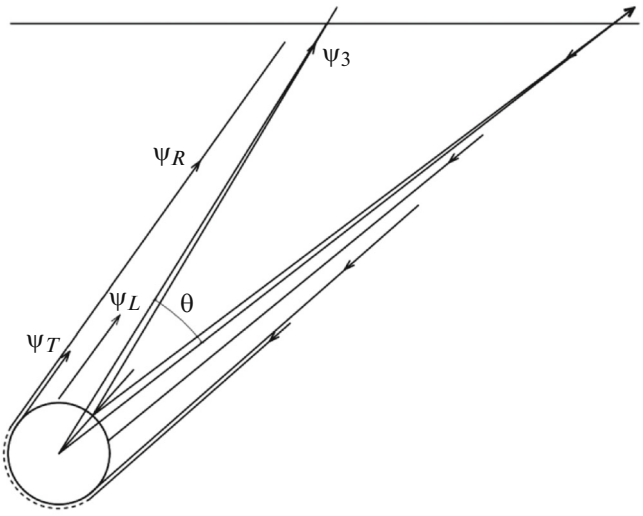

Fig. 10. Specular reflection and rounding an SDH by transverse waves.

Thus, corner and segmental reflectors also have limitations in ensuring the necessary accuracy of orientation and size, as well as possible changes in material properties during their manufacture. Therefore, the following question is relevant: is it possible to use a simpler reflector?

In this regard, let us return to the configuration of an SDH. First, extended drillings of various orientations are easy to manufacture and calibrate, including under ongoing production conditions. At the same time, the acoustic properties of the sample material are practically not violated, and this is an obvious advantage of such a reflector over a notch. Secondly, on the cylinder, the scattering diagram (indicatrix) in the specular reflection zone is almost circular, and the intensity of the diffracted wave incident along the cylinder at the "cylinder—bottom" intersection is less than on the notch. Third, an SDH or vertical drilling has no ends and side edges, i.e., the resulting signal is formed more easily than on a notch or a flat-bottomed hole.

Some time ago, according to the paper [35], it was believed that small dimeters should not be used to adjust the sensitivity of ultrasonic testing, since the amplitude of the received signal oscillates when the cylinder diameter changes. However, it was shown in [36, 37] that these oscillations occur only if the signals mirrored from the drilling surface interfere with the envelope signals (Fig. 10), moreover, according to [38], the delay time of the envelope signal is calculated by the formula:

$$\delta_d = 2b_{\text{SDH}}\left\{\frac{\cos\frac{\Delta}{2}}{c_{\text{T}}} + \frac{\pi}{2c_{\text{R}}}\left(1 - \frac{\Delta}{180}\right)\right\}, \tag{5}$$

where $2b_{\text{SDH}}$ is the SDH diameter, Δ is the angle between the direction to the source and receiver of ultrasonic waves (in deg), c_{T} and c_{R} are the velocities of a transverse and Rayleigh wave.

Currently, the duration of ultrasonic pulses at frequencies of 2.5 MHz and higher does not exceed 1–2 μs. At the same time, it follows from (5) that these signals are almost always resolved in time and do not distort each other when sounding a SDH with a diameter of 2 mm or more by a transverse wave, and the amplitude of each of them changes monotonously when the drilling diameter changes. For example, the amplitude of a specularly reflected signal varies according to the law [24]

$$A_{\text{SDH}} \sim \frac{(b_{\text{SDH}})^{\frac{1}{2}}}{\lambda r^{\frac{3}{2}}}. \tag{6}$$

This dependence is taken as a basis for setting the sensitivity of an SDH with a diameter of 6 mm in the SO-2 block, which, according to SKH diagrams introduced by professor A.K. Gurvich that link the equivalent area of the defect with its signal detectability, varies according to the law in [1, 29].

An example of an estimate for (6) is the blue curve in Fig. 7. Since the dependence (6) is more smooth than in (3) for a flat-bottomed drilling, the accuracy of sensitivity adjustment for through drilling may be lower than for a flat-bottom hole. However, for small-diameter SDHs (for example, $d_{SDH} = 2b_{SDH} = 2$ mm) when testing small thicknesses, when the distances r are small, it follows from (3) and (6) that the dependence $A(r)$ remains steep enough to ensure the accuracy of sensitivity settings within 1 dB.

Thus, the simplicity of manufacturing and checking the parameters of SDHs allows one to focus more on this reflector. It is SDHs that are recommended in foreign standards [39, 40] for constructing distance–amplitude curves (DAC curves). However, it should be remembered that when sorting defects based on equivalent area, the testing sensitivity must be recalculated taking into account the relationship between the amplitudes in (3) and (6).

Note that the time delay δ_d between the mirrored and the most significant envelope of SDH signals can be used to verify and adjust the depth gauge scale and time scale [36, 38]. For example, for a combined transverse wave input scheme with an angle ultrasonic transducer, i.e., for $\Delta = 0$, from (5) we obtain

$$\delta_d = Eb_{SDH}, \tag{7}$$

where b_{SDH} is given in millimeters, and δ_d is in microseconds. The constant coefficient can be somewhat refined for each specific material. If the drilling diameter is set with an error of 0.1 mm, then the time interval is determined from (7) with an error of no more than 0.1 μs.

Let us also consider a vertical cylindrical reflector, for example, a through hole. According to [24, 41], the amplitude A_{BC} of the signal specularly reflected from it and received by an angle single crystal prove with entry angle α is determined by the relation

$$A_{BC} \sim \frac{N_{BC}}{\sin\alpha}\frac{(b_{SDH})^{\frac{1}{2}}}{\lambda r^{\frac{3}{2}}}, \tag{8}$$

where the coefficient $N_{BC}/\sin\alpha$ is similar to the coefficient N for the notch in (4); it takes into account the possible influence of the bottom surface. Using (8) in conjunction with (3), the sensitivity of the vertical drilling setting can be recalculated compared to the flat-bottomed drilling setting.

Note that vertical drilling is universal in the sense that its intersection with the sample surfaces simulates defects coming to the product surfaces, and the central part is internal defects. Therefore, the same drilling can be used on straight and reflected beams in a "tandem" scheme and in a "chord" or any other scheme in which the input and/or output planes of ultrasonic waves do not coincide with the plane of Fig. 6 (see, for example, [1, 42, 43]). It should only be remembered that the SDH in the SO-2 block is sounded perpendicular to the cylinder axis, i.e., we have a two-dimensional problem of ultrasonic wave scattering by a cylindrical cavity, while 3D scattering is implemented for vertical drilling—the directions of sounding are not perpendicular to the cylinder axis [44, 45], and it may be necessary to adjust the calculation of scattered signals.

Also note that, as shown in [38, 45], the amplitude due to the drilling signal in a wide range of angles and material properties is proportional to the angle of inclination of the cylinder axis. This makes it possible to reduce the influence of the slopes of the drilling axis on the results of setting the ultrasonic testing parameters. For example, the sensitivity can be adjusted by the half-sum of the amplitudes A_1 and A_2 of the echo signals received from the drilling in opposite directions, as in Fig. 11,

$$A = \frac{A_1 + A_2}{2}. \tag{9}$$

The value of A with an error of less than ±0.75 dB is equal to the nominal amplitude of the echo signal from a cylindrical drilling performed strictly vertically.

From the above, it is obvious that the metrological support of ultrasonic testing when using drilling in various directions in samples is much easier to implement than for other reflectors discussed in this section. It seems advisable to use these reflectors more widely, including vertical drilling, when revising the current standard [17].

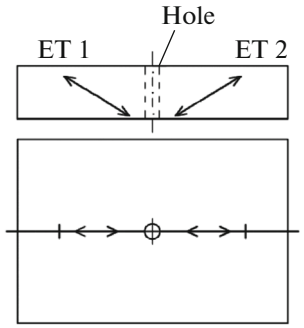

Fig. 11. On the adjustment of sensitivity for vertical drilling.

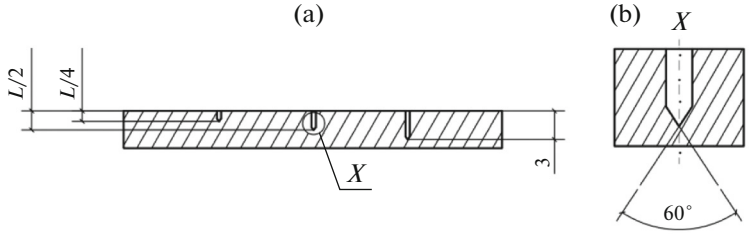

Fig. 12. Fragment of a tuning sample with grooves according to [47]: (a) general appearance, (b) regulated groove shape.

SLOTS IN THE TUNING SAMPLES

Concluding the above review, it is necessary to consider the use of slots as reflectors. They were mentioned above in connection with checking the resolution of the transducer–flaw-detector system based on the SO-1 and V1 calibration blocks. Let us look at this reflector from a different point of view. More precisely, it is not entirely correct to talk further about the groove as a reflector, since we will talk more about diffraction effects, for example, the diffraction-time method (TOFD—time-of-flight diffraction) [6, 46]. In the standards, including foreign ones, operating approximately since 1998, for example, in [47], the signal scattered by the tip of a groove is used to adjust the scan range. In this case, the opening of the groove is stipulated, for example, 0.2 mm, and the angle between the edges at the tip is 60° (Fig. 12). However, what is this tip and how to make a groove to meet the requirements for its geometric shape?

Obviously, when milling, the end of the groove has a natural rounding. Its diameter can be reduced if the groove is made using an electroerosion method. Nevertheless, even in this case, the end has the form of a half-cylinder (Fig. 13).

In TOFD, the main analyzed characteristic is not the amplitude of signals, but the time of their reception. When the groove opening is fractions of a millimeter, this time can be recorded within approximately 0.1 μs, a value that is sufficient to measure the coordinates of the tip in steel or aluminum with an accuracy of 0.6 mm on a longitudinal wave or 0.3 mm on a transverse one. A different situation occurs when analyzing the amplitudes of signals due to slots. At a frequency of 5–10 MHz, the diameter of the rounding of an electroerosion groove is close to 0.4 wavelength. Experimental results indicate that the angular dependences of the amplitudes of the signals scattered by such curves are similar to the scattering by an SDH, and not by the tip of the half-plane simulating a crack [48]. Therefore, the amplitude of the signal scattered by the groove end, even with the minimum achievable opening, cannot be used to assess the presence or absence of a tip in a real defect. The reason becomes obvious if we compare Fig. 13 with Fig. 14, which shows microetches of steel samples with cracks on a similar scale: the crack opening is considerably smaller even with the smallest opening of grooves.

Also note that in the standards [6, 47], it is proposed to complete grooves (cuts) by a small diameter drilling. According to the above, such a drilling with a diameter of no more than 2 mm allows one to set the time for receiving signals around the cuts with an accuracy of 0.1 mm. However, in this case, ultrasonic waves bend around the drilling according to a mechanism similar to that depicted in Fig. 10 for a volumetric defect. Therefore, as for Figs. 12 and 13, the amplitude of the recorded signals does not correspond to the amplitude of signals that envelope the crack tips.

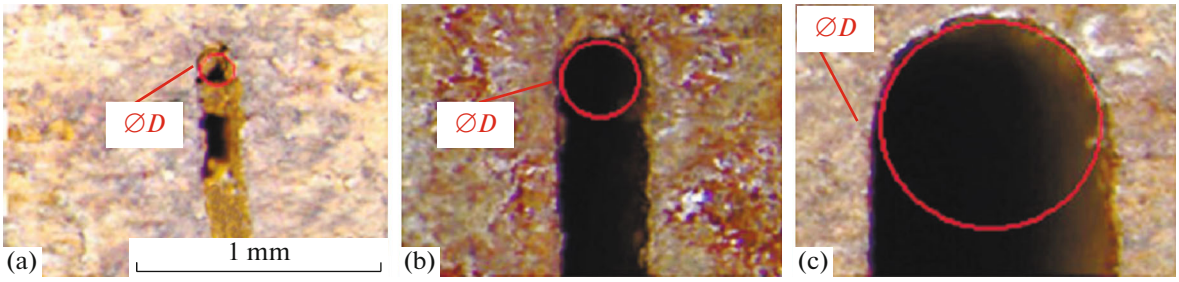

Fig. 13. Macrosections of grooves with a width of 0.14 (a), 0.4 (b), and 1.0 (c), made by the electroerosion method [48].

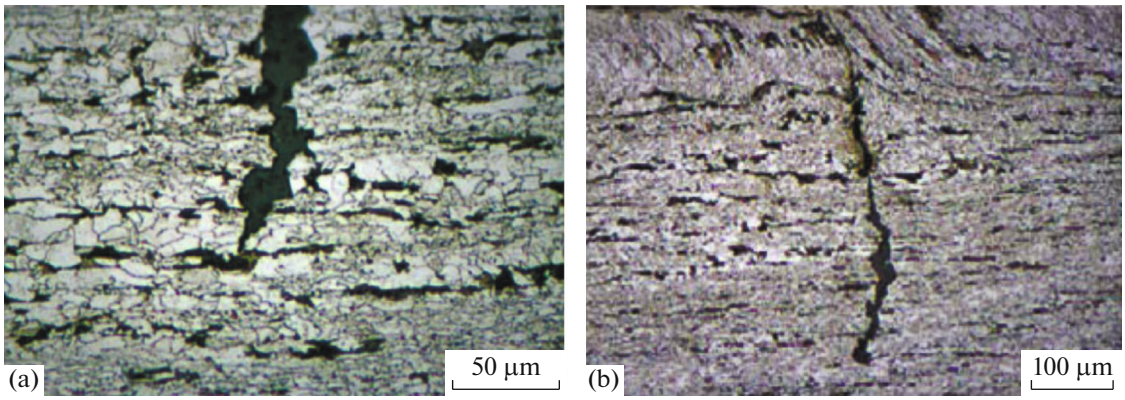

Fig. 14. Cracks in the section of the pipe wall [49, 50]; scale: (a) 1 cm = 50 μm, (b) 1 cm = 100 μm.

It seems advisable to take into account the above features of ultrasonic wave scattering by grooves during the next revision of the standard [17].

ON MODELING DEFECTS IN AUTOMATION OF SCANNING

Next, we will consider the prospects of using various artificial reflectors to adjust the parameters of ultrasonic testing taking into account the automation of scanning, digital signal processing, and presentation of information about defects in product cross-sections. One example was given to illustrate the possibility of measuring the thickness of a product using B-scan. Figure 15 shows another example of an image of a metal cross-section: an S-scan of a butt weld with a thickness of 9 mm obtained by a phased array antenna (PAA) with entry angles in the range 45°–70°. When superimposing this image on the cutting edges, it can be seen that signals 1.1 and 1.2 on straight and reflected beams are obtained from lack of fusion 1 and signal 2, on straight beam from slag inclusion 2.

Conventionally, it is assumed that the amplitude of the signal from a planar defect should be greater than from a volumetric one with a similar aperture. In Fig. 15, the maximum amplitude corresponds to the red color, i.e., the relationship of amplitudes is inverted. Obviously, the reason is that the lack of fusion is sounded in a suboptimal way.

In this regard, let us return to considering artificial defects in the samples to adjust the parameters of ultrasonic testing. When constructing DSG diagrams "manually," the transducer is set by small offsets and rotations so that the amplitude of the echo signal from the flat bottom in Fig. 6a takes the maximum possible value. However, with automated testing, it is often not possible to search for the maximum amplitude of the signal from each defect. Figure 16 shows an example of B- and C-scans due to flat-bottomed holes during automated movement of the transducer over the surface of the tuning sample. Now the maximum amplitude value for each reflector is at least not obvious.

On the one hand, when checking welds, certain deviations of the testing parameters from the nominal values are allowed [8, 17, 50–52]. However, on the other hand, in practice such deviations can be very considerable [53–55]. It was shown in [56, 57] that with an acceptable change in the frequency of ultrasonic waves within ±10% or the entry angle by ±3°, the amplitude of the signal due to a flat-bottomed

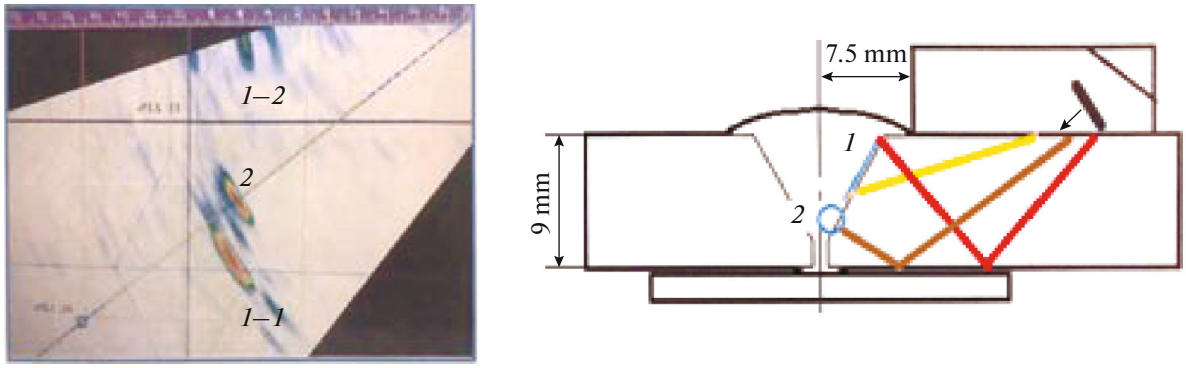

Fig. 15. S-scan of a weld.

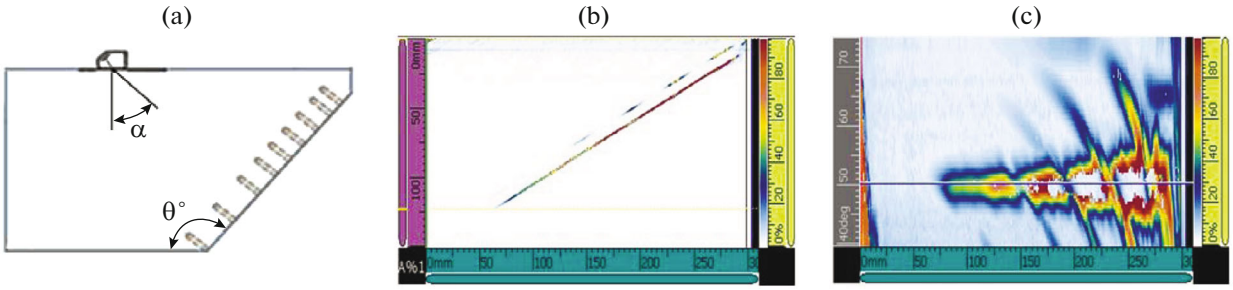

Fig. 16. Result of scanning a sample with flat-bottomed holes: (a) layout of flat-bottomed holes, (b) B-scan, (c) C-scan [58].

drilling is measured up to ±2 dB in the first case and up to ±3.5 dB in the second case (Fig. 17). Thus, even in the traditional echo method, errors of two times or more are possible when setting sensitivity and then when measuring the equivalent area of defects.

Similarly, for the notch: when the transducer is shifted from the calculated position by 1–2 mm, the amplitude of the received signal may change by 6 dB, i.e., the measured equivalent area may differ from the design one by 2 times. However, this is exactly the situation that occurs when scanning products in automated mode: by moving the transducer along the weld, the operator usually sounds the defect in a "nonoptimal" direction.

If, according to the operating conditions of the facility, it is mandatory to increase the accuracy of localization of defects, then detailed scanning with duplication in automated or manual modes can be economically justified. Nevertheless, at the same time, the testing performance may decrease considerably. More often it is not possible to repeat the scan. This is the case, for example, when diagnosing welds of main pipelines, reservoirs, etc. Therefore, it is necessary to evaluate defects under conditions where acoustic images obtained during a single scan cycle do not provide measurement of the maximum values of signal amplitudes. It is also important that as ultrasonic flaw detection technology develops, it is necessary to increase the degree of automation of image decoding [9]. Therefore, the questions posed seem relevant for further development of flaw detection in general and, in particular, the applied methods and technologies of ultrasonic testing.

The simplest situation arises if new signals are detected during the next inspection cycle, which can be interpreted as signals from defects that occurred in the product during the interdiagnostic period. In this case, the amplitude is of auxiliary value. The fact of the defect occurrence itself is more important. It is necessary to determine whether it is mechanical damage, crack, or corrosion. If the type of defect is determined, then it is possible to analyze the cause of its occurrence and the rate of development and plan the period and conditions for continued operation or the period of withdrawal of the object for repair.

A more difficult case is if the examination reveals a change in the parameters of previously detected signals, for example, the amplitude or conditional length has increased. However, a downward change

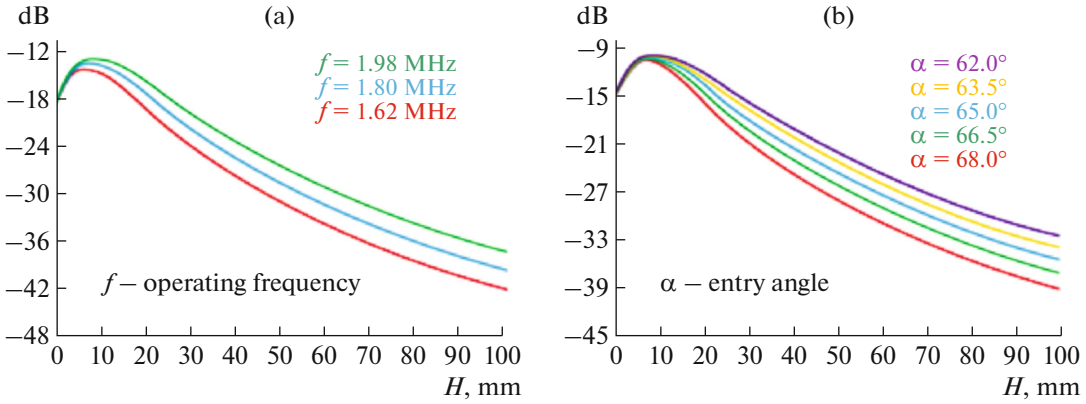

Fig. 17. Influence of frequency (a) and entry angle (b) on the parameters of DGS diagrams [56].

is also possible. Then, in order to make any decisions, it is necessary to determine how significant the detected change is and whether it fits within the limits of measurement error. Let us explain this using an example developed according to [8] to link the size of a defect in the product to the period during which the operation of the object can continue (Fig. 18). The defect dimensions measured during ultrasonic inspection are plotted along the axes; curve *1* sets the maximum permissible sizes of defects, and the following areas of safe operation are introduced: *2* at the end of the evaluation period and *3*, *4*, and *5* for one, two, and four years, respectively. It can be seen that in this case, the difference in the height of defects transferring them from one category to another is 2 mm. Nevertheless, from the same source [8] it is known that the error in measuring the height of a defect (or the depth of its tip in the weld) is close to the wavelength of the ultrasonic wave. Therefore, for a transverse wave at a frequency of 2.5 MHz, i.e., with a wavelength of 1.2 mm in steel, the error in measuring the height of the defect is at least ±1.2 mm. For example, if the measured height of the defect is 5.5 mm with a conditional length of 50 mm, then it follows from Fig. 18 that a product with the defect can be used for up to two years. However, taking into account the specified error, the height of the defect is in the range from 4.3 to 6.7 mm. Therefore, the permissible service life of the product should be reduced to one year. By measuring the coordinates of the defect tip with the smaller error, it would be possible to more accurately assess the safe operation of the object or set smaller margin coefficients.

Figures 19a and 19b shows another example from the collection in [8]: B- and D-scans of the same detected defect, i.e., its ultrasound images in the cross section of the weld and in the section along the axis of the seam. It follows from the image of the microsection in Fig. 19c that a crack has been detected. However, it is necessary to pay attention to the fact that along the vertical axis in the B- and D-scans, the scale is constructed in 6 mm increments. The question arises: on which section of the D-scan and with what accuracy was its height measured? After all, if one moves the transducer a few millimeters along the axis of the weld, then when estimating the height of the defect, one can make a mistake of ±2 mm relative to the image shown in the B-scan on the left. In this case, the amplitude of the signal due to the defect can either increase or decrease, leading to uncertainty in the assessment of the safe operation period of the object according to the diagram in Fig. 18. Therefore, as mentioned above, when analyzing images of defects in the cross section of products, it should be borne in mind that the amplitude of the received signals is an important, but not the only, and sometimes not the main parameter that needs to be analyzed when measuring the dimensions and presorting defects.

On the one hand, the above acoustic images of defects illustrate the significant progress that has occurred in ultrasonic flaw detection since the beginning of the 21st century. Indeed, ultrasonic flaw detection technologies have been developed and introduced into production, allowing one to visualize the position of defects in the cross section of products and welds. On the other hand, it seems that at present the metrological support of ultrasonic testing methods, in particular, the accuracy of measuring defect parameters from the obtained images lags behind these technologies themselves. For example, an urgent question arises about how to properly configure the parameters of automated ultrasonic testing when the detection and presorting of defects is carried out within a continuous measurement cycle [9]. Apparently, additional technological techniques are required to clarify the parameters of detected defects.

Here are examples from related fields of science and technology. For example, it is well known that dolphins (bottlenose dolphins) use echolocation for orientation, search, and communication in the water.

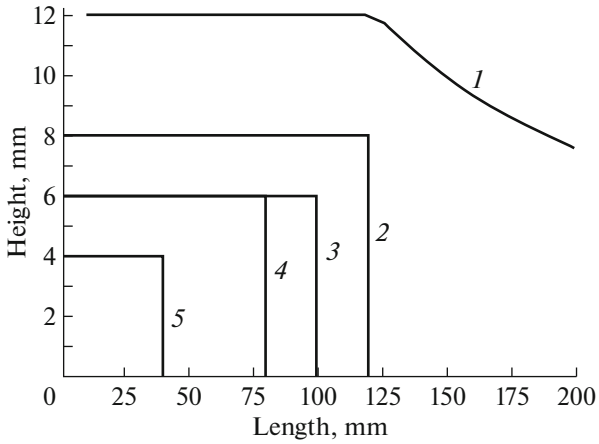

Fig. 18. Diagram of permissible defect sizes.

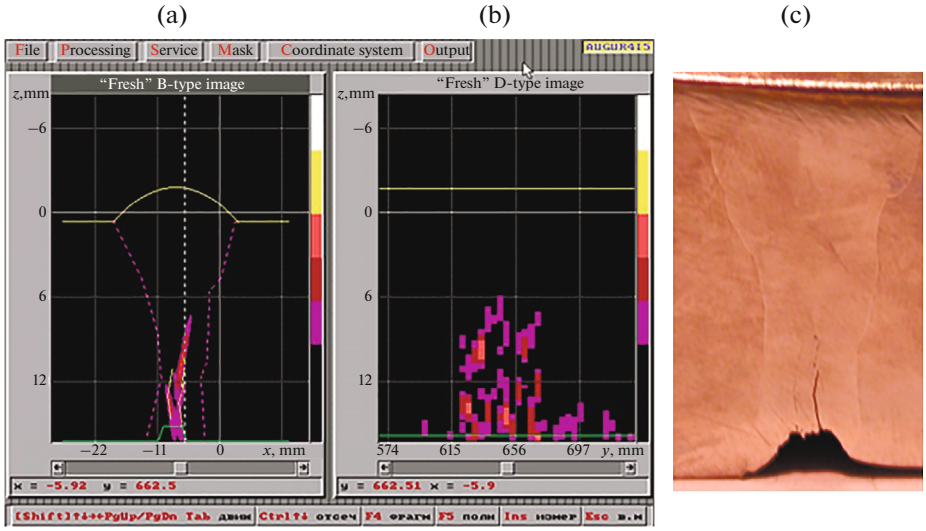

Fig. 19. B- and D-scans in comparison with the microsection of a real crack [8].

Researchers working in this field believe that dolphins use four different ways of sounding objects at different frequencies, from different directions, and with different emission and reception patterns. As a result, a four-dimensional image of the environment is formed, including three spatial coordinates and the spectral composition of the received signals. This makes it possible, for example, to distinguish between two balls of the same materials the diameters of which differ by 2–3% or two objects of the same shape with a density difference of 10% [13].

Another example is ultrasound scanning during medical examination of human soft tissues [14]. Frequencies in the range from 1 MHz (wavelength 1.5 mm) to 6 MHz (wavelength 0.4 mm) are usually employed. However, to measure the thickness of individual structures, for example, the membranes of organs or skin, the frequency can be increased to 12 MHz, a value that corresponds to a wavelength of 0.2 mm. Several techniques are used, including comparing the results of sounding organs from different directions. As a result, experts establsih the size of objects starting from approximately 0.2 mm.

There are several significant differences in the conditions of echo location in the examples given and in ultrasonic flaw detection. First, there are no transverse waves in the liquid, and therefore the amount of interference of acoustic origin is less than in the examination of elastic media. Second, for the specified areas of application of ultrasonic location, the detection of cracks and the measurement of curvature at the object tip is not a typical task. Finally, both for dolphins and in medicine, the echogenicity of the

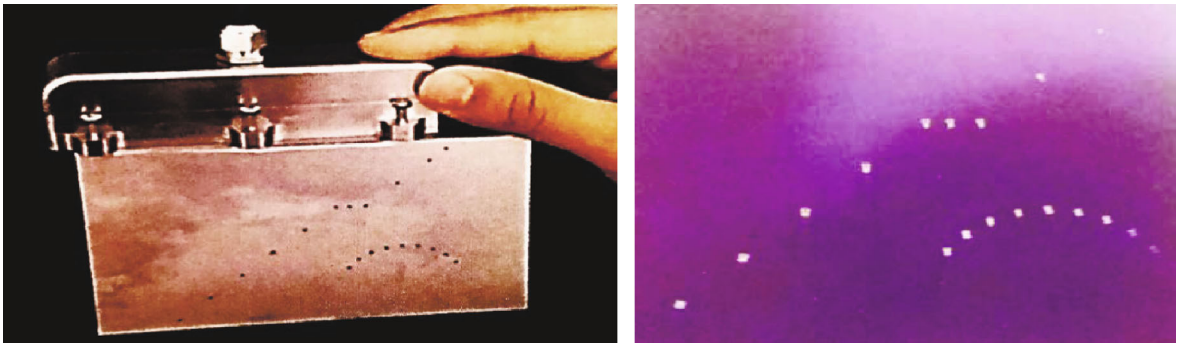

Fig. 20. Detection of an SDH in a steel sample using FMC/TFM [61].

internal structure of the examined "organ" is important: whether it is homogeneous and whether additional elements are allocated in it. In ultrasonic flaw detection, the internal structure of a crack or slag inclusion is usually not of interest.

However, we emphasize that the most important common feature of the above examples that may be important for ultrasonic flaw detection is the fact that the observed objects are evaluated only by comparing acoustic images obtained via different channels or from different directions and after comparing them with the "norm." At the same time, the amplitude of received signals is an important but not the main parameter being analyzed.

The development of ultrasonic flaw detection in general is also moving in this direction. An example are technologies using multielement systems with synthesized aperture—digital focusing of the antenna array (DFA) [59, 60]. In foreign practice, the abbreviation FMC/TFM (Full Matrix Capture/Total Focusing Method is full matrix capture in combination with the total focusing method) has been established for systems of the kind [61]. These methods are based on the fact that each of the antenna array elements (or some group of its elements) emits ultrasonic waves, and each element of the array (or some group of elements) receives signals scattered by a defect. The overall dimensions of the antenna array are usually in units of centimeters, i.e., defects with a length or height of millimeters are sounded from different sides, and the software "collects" all scattered signals taking into account their amplitudes, phases, and reception time bias.

Figure 20 illustrates the acoustic image of a SDH with a diameter of 1 mm obtained using the FMC/TFM method. The drilling coordinates can be determined within 1 mm. Similar images of volumetric defects can be found in [8, 59] and other sources. Nevertheless, the question arises: what do acoustic images of planar defects look like? A possible answer is given, for example, in [62]. Using special processing algorithms based on the DFA method, the authors obtained acoustic images of a slit with a width of less than 1 mm and a depth of 4 mm in a 17 mm thick sample made of St20 steel in comparison with the image of an SDH with a diameter of 1.5 mm, Fig. 21.

On such tomograms, the image of a planar defect (groove) can be correlated with its actual shape. The effect is enhanced if the image of the defect is simultaneously fixed in a perpendicular section, as in Figs. 19a and 19b. However, according to the images in Figs. 15, 19, and 21, the opening and coordinates of the "tip" of the real or "artificial" defect can only be estimated within 2–3 mm, depending on the sensitivity level at which the measurement is taken. This natural limitation is connected with the relationship between wavelength, pulse duration, and achievable resolution. Moreover, the image of real cracks on tomograms, in comparison with images of artificial defects (grooves), can be further expanded due to the scattering of ultrasonic waves by the rough surface of the defect inclined with respect to the surfaces of the product [5, 63].

Thus, at present, it can hardly be assumed that the measurement error of the opening of planar defects by ultrasound tomograms is sufficiently small to confidently estimate the coordinates of the tip and the opening of planar defects with an error of less than a millimeter. In fact, the decision on the opening of a crack is made on the basis of an expert assessment after training a specialist (or an automated system) using databases of images of artificial and real cracks and other defects. In order to make full use of the information that B-, C-, D-, and other scans currently allow, it is necessary to develop and accumulate digital models of products, welds, and tuning samples with and without artificial and real defects of vari-

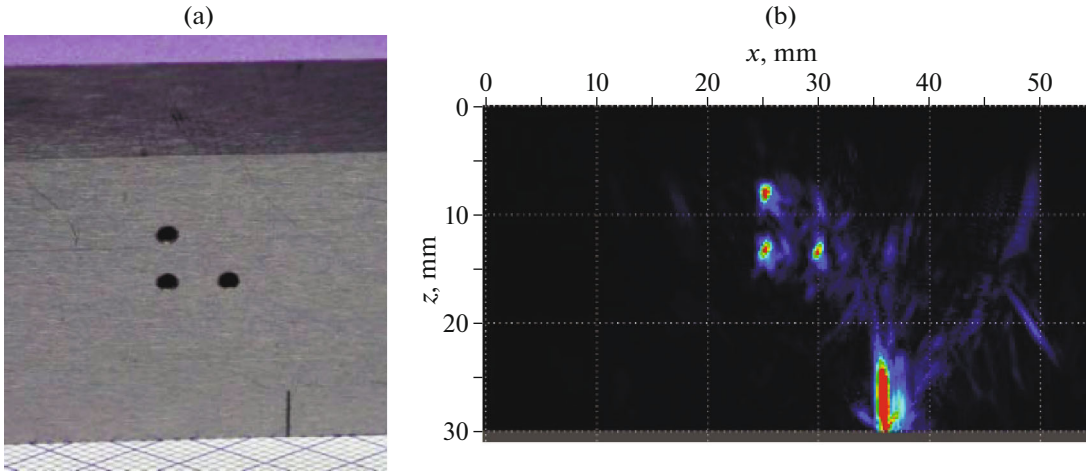

Fig. 21. Identification of an SDH with a diameter of 1.5 mm and a vertical groove with a depth of 4 mm using DFA [5].

ous types. To automate the measurement of the opening and dimensions of defects based on their acoustic images, it is necessary to take into account:

– The size and orientation of artificial defects (grooves, drillings).

– The shape of the defect image in acoustic images taking into account the sounding of the defect from different directions.

It also seems advisable to analyze the spectrum of received signals. The amplitude of the signals in acoustic images is also important but much less than it used to be in the analysis of A-scans.

CONCLUSIONS

1. Calibration blocks (measures) SO-2, SO-3, and alike, as well as tuning samples with artificial defects are designed to determine the maximum achievable characteristics of equipment for ultrasonic testing and to adjust this equipment.

2. Depending on the field of application and the type of tested products, tuning samples with artificial and/or natural defects are used when setting the ultrasonic testing parameters. Such "defects" can only be conditionally called the traditional word "reflector," since diffraction effects often make the main contribution to the recorded signals.

3. Among the artificial defects ("reflectors"), the bottom surface (flat and cylindrical), flat-bottomed drillings, SDHs (side drilled holes), and corner reflectors ("notches") are the most widespread in domestic practice. In foreign practice, grooves are used to a greater extent. Also, grooves and SDHs are used for testing using the ultrasonic diffraction-time method TOFD.

4. Vertical drilling is rarely used during setup; the advantages of this reflector when working with the echo method are underestimated. Meanwhile, measures and tuning samples with artificial defects ("reflectors") in the form of drillings are the easiest to produce and confirm their metrological characteristics. Using simple technological techniques, it is possible to considerably reduce the influence of random deviations in the orientation of drilling and acoustic properties of the material on the results of setting the ultrasonic testing parameters. It seems advisable to recommend expanding the use of cylindrical drillings of various orientations, as well as grooves, during the next revision of the standards for ultrasonic testing.

5. At the present stage of development of ultrasonic flaw detection, the term "defect modeling" should be understood not in the previously traditional sense of "which models of artificial defects are best to use" but in the sense that the methods and technology of equipment tuning and methods of processing the information received, including the use of tuning samples, should allow one to identify the defect and measure it parameters with the accuracy necessary to calculate the strength, stability, residual life, and other operational characteristics of the structure. Ultrasonic inspection technology should provide measurement of the size, shape, and orientation of defects. To achieve this goal, it is necessary to train (specialists and/or automated systems) using digital "twins" of tuning samples with defects that can be obtained, for example, by applying digital focusing of the antenna array (DFA or FMC/TFM).

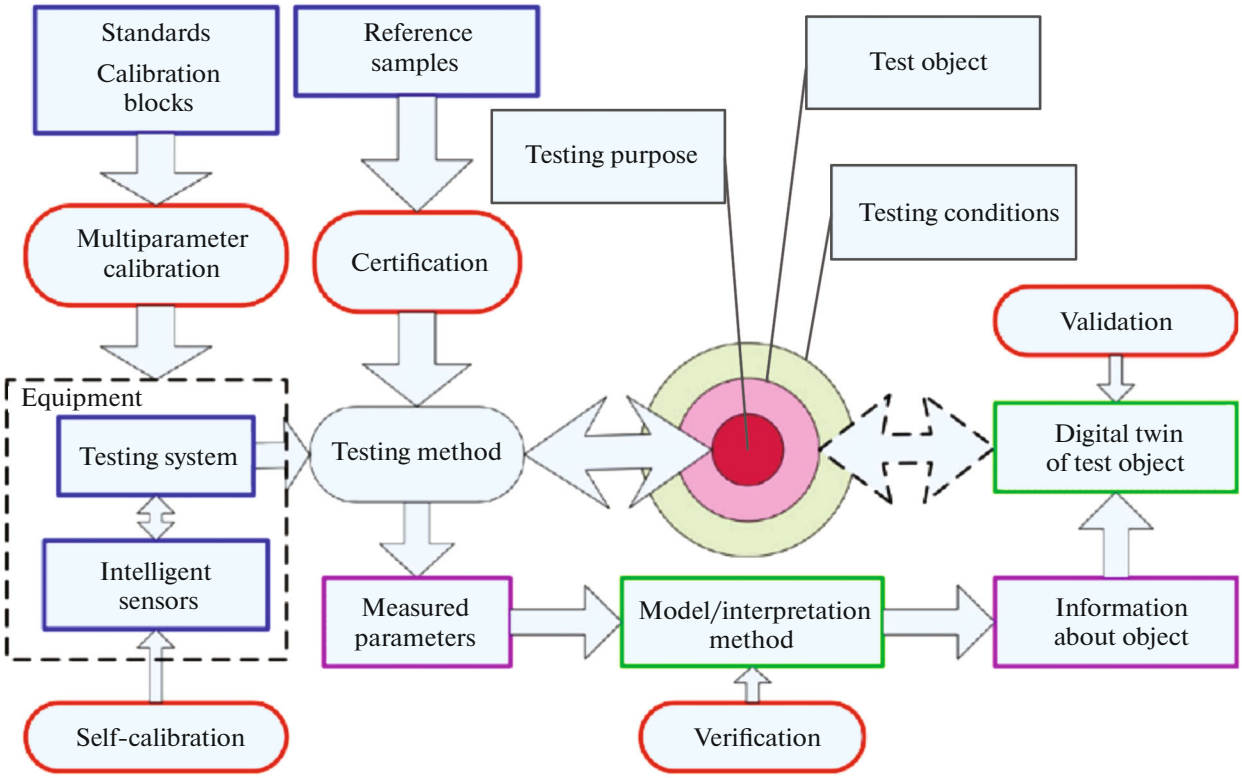

Fig. 22. General quality control scheme [9, 64].

6. Taking into account modern trends in the construction of nondestructive testing equipment and the formed tasks of automatic interpretation of measurement information in order to determine the type of structural defects (discontinuities) and their geometric parameters, the general scheme of a nondestructive testing (flaw detection) system and the conditions for performing technological operations, including as part of the work on the diagnostics of technically complex systems, is shown in Fig. 22, according to [9, 64]. Within the framework of this scheme, it is necessary to ensure validation (confirmation of compliance with specified requirements) of digital models of defects and the test object, verification (approbation) of testing methods, and performing of testing with automation of various operations. Such operations may include (all or some): calibration and adjustment of equipment by detecting artificial and/or real defects in tuning samples, scanning, transmitting and recording primary results, decoding the acoustic images obtained, presorting each identified defect and the product as a whole, and archiving data.

7. The decision on the size, shape, orientation of defects identified based on the acoustic images shown in Figs. 15, 16, and 19–21 or on similar ones obtained using other visualization methods should be based on a comparison of the acoustic image of defects in the tested product with the "digital twins" of the tuning sample with artificial and/or actual defects and relevant regulatory and technical documentation. The same is true to obtain information about developing defects. At the same time, one should remember about possible limitations on the accuracy of measuring the size of the opening and the coordinates of the defect within 2–3 mm, depending on the set sensitivity level. This natural limitation is related to the relationship between wavelength, pulse duration, and achievable resolution.

8. Currently, the evaluation of defect parameters for B-, C-, D-, and other scans is performed at the expert level by highly qualified specialists. To automate this process, it is necessary to accumulate a representative sample of acoustic images ("digital twins") of tuning samples and tested products with and without defects.

9. It is necessary to develop unified approaches to the certification of digital twins of tuning images with and without defects [9]. If this operation is performed on equipment from one company, it may not be possible to view and analyze these results on other equipment. Therefore, it is advisable to switch to a single standard for the presentation of data obtained during ultrasound testing. For example, the DICONDE format (Digital Imaging and Communication in NDE) is known [6, 65]. However, it is designed by anal-

ogy with the DICOM format used in medicine (Digital Imaging and Communication in Medicine), which is primarily focused on working with flat images. This is not sufficient for ultrasonic flaw detection, since it is necessary to store all types of scans, including A-scans that are irrelevant for radiography. Perhaps the best solution would be to use other proposals, for example, [66], if this allows describing the entire set of information necessary for receiving, processing, storing, archiving, transmitting, and receiving acoustic images of reflectors, tuning samples, and tested products in a universal way compatible with equipment from different manufacturers.

FUNDING

This work was supported by ongoing institutional funding. No additional grants to carry out or direct this particular research were obtained.

CONFLICT OF INTEREST

The authors of this work declare that they have no conflicts of interest.

REFERENCES

1. Aleshin, N.P., Belii, V.E., Vopilkin, A.Kh., Voshchanov, A.K., Ermolov, I.N., and Gurvich, A.K., *Metody akusticheskogo kontrolya metallov* (Methods of Acoustic Testing of Metals), Moscow: Mashinostroenie, 1989.
2. Ermolov, I.N. and Lange, Yu.V., Ultrasonic monitoring, in *Nerazrushayuschii kontrol': spravochnik v 8 tomakh* (Nondestructive Testing: A Handbook in 8 Vols.), Klyuev, V.V., Ed., Moscow: Mashinostroenie, 2008, vol. 3.
3. Krautkramer, J. and Krautkramer, H., *Werkstoffprufung mit Ultrachall,* Berlin: Springer, 1986.
4. Badalyan, V.G., Bazulin, E.G., Vopilkin, A.Kh., Kononov, D.A., Samarin, P.F., and Tikhonov, D.S., *Ul'trazvukovaya defektometriya metallov s primeneniem golograficheskikh metodov (Ultrasonic Metal Flaw Detection Using Holographic Methods)*, Vopilkin, A.Kh., Ed., Moscow: Mashinostroenie, 2008.
5. ACS Company official web-site. https://acsys.ru/vozmozhnosti-otsenki-kharactera-nesploshnosti-metall-aultrazvukovym-tomografom. Accessed December 18, 2023.
6. Ginzel, E., *Ultrasonic Time of Flight Diffraction,* Waterloo: Eclipse Sci., 2013.
7. Ginzel, E., *Phased Array Ultrasonic Technology,* Waterloo: Eclipse Sci., 2013.
8. *Ul'trazvukovaya defektometriya. 30 let: Yubileinii sbornik trudov OOO NPTs EKhO+ (Ultrasonic Flaw Detection. 30 Years: The Jubilee Collection of Works of NPC Echo+ LLC)*, Vopilkin, A.Kh., Ed., Moscow: Spektr, 2020.
9. Gogolinskii, K. and Syas'ko, V., Metrological assurance and standardization of advanced tools and technologies for nondestructive testing and condition monitoring (NDT4.0), *Res. Nondestr. Eval.,* 2020, no. 31, pp. 325–339. https://doi.org/10.1080/09349847.2020.1841863
10. Syas'ko, V. and Gogolinskii, K., From NDT to Condition Monitoring, *Dev. Trends Digital Econ.,* 2020, no. 23, pp. 4–8. https://doi.org/10.12737/1609-3178-2020-4-8
11. Mogil'ner, L.Yu., Neganov, D.A., and Skuridin, N.N., *Obsledovanie metallokonstruktsii na ploschadochnykh ob'ektakh magistral'nykh truboprovodov* (Inspection of Metal Structures at Site Facilities of Main Pipelines), Moscow: Tekhnosfera, 2023.
12. Kretov, E.F., *Ul'trazvukovaya defektoskopiya v energomashinostroenii* (Ultrasonic Flaw Detection in Power Engineering), St. Petersburg: Sven House, 2014.
13. https://stena.ee/blog/rfr-eto-rabotaet-eholokatsia-delfinov. Accessed December 18, 2023.
14. https://evromedcompany.ru/ultrazvuk/rukovodstvo-po-ultrozvuk. Accessed December 18, 2023.
15. Syas'ko, V. and Shikhov, A., Assessing the state of structural foundations in permafrost regions by means of acoustic testing, *Appl. Sci.,* 2022, no. 12, p. 2364. https://doi.org/10.3390/app12052364
16. Ogino, T., Kawaguchi, T., Yamashita, S., and Kawajiri, S., Measurement deviations for shear wave velocity of bender element test using time domain, cross-correlation, and frequency domain approaches, *Soils Found.,* 2015, no. 55, pp. 329–342. https://doi.org/10.1016/j.sandf.2015.02.009
17. *GOST* (State Standard) *R 55724-2013.* Nondestructive testing. Welded joints. Ultrasonic techniques, 2013.
18. *ISO 2400.* Nondestructive testing—Ultrasonic examination—Specification for calibration block no. 1, 2012.
19. *ISO 7963.* Nondestructive testing—Ultrasonic examination—Specification for calibration block no. 2, 2022.
20. Murav'ev, V.V., Zuev, L.B., and Komarov, K.L., *Skorost' zvuka i struktura stali i splavov* (Speed of Sound and Structure of Steel and Alloys), Moscow: Nauka, 1996.

21. Rinkevich, A.B. and Smorodinskii, Ya.G., Elastic waves in an inhomogeneous austenite plate in the model of a transversely isotropic medium, *Russ. J. Nondestr. Test.,* 2001, vol. 37, no. 7, pp. 475–495.
22. Aleshin, N.P., Baranov, V.Yu., Bezsmertny, S.P., and Mogil'ner, L.Yu., The effect of the anisotropy of the elasticity of rolled products on the detection of defects during ultrasonic quality control of welding of large diameter pipes, *Defektoskopiya,* 1988, no. 6, pp. 80–86.
23. *Ul'trazvukovye p'ezopreobrazovateli dlya nerazrushayushchego kontrolya* (Ultrasonic Piezoelectric Transducers for Nondestructive Testing), Ermolov, I.N., Ed., Moscow: Mashinostroenie, 1986.
24. Ermolov, I.N., *Teoriya i praktika ul'trazvukovogo kontrolya* (Theory and Practice of Ultrasonic Testing), Moscow: Mashinostroenie, 1981.
25. Konshina, V.N. and Dymkin, G.Ya., Modern approaches to the certification of ultrasonic testing techniques, *Russ. J. Nondestr. Test.,* 2008, vol. 44, no. 2, pp. 77–85.
26. *GOST* (State Standard) *8.495-83.* State system for ensuring the uniformity of measurements. Ultrasonic contact thickness gauges. Methods and means of verification, 1983.
27. htts://constanta-us.com/catalog/nabor_kusot_180). Accessed January 15, 2024.
28. Mogil'ner, L.Yu., Skuridin, N.N., Pridein, O.A., and Timeko, A.I., The use of electromagnetic-acoustic thickness gauges in diagnostics of metal structures and mechanical-technological equipment, *Nauka Tekhnol. Truboprovodn. Transp. Nefti Nefteprod.,* 2019, vol. 9, no. 3, pp. 315–325.
29. *GOST* (State Standard) *14782-86.* Nondestructive testing. Welded joints. Ultrasonic methods, 1988.
30. *GOST* (State Standard) *R ISO 5577-2009.* Nondestructive testing. Ultrasonic testing. Glossary, 2009.
31. Ermolov, I.N., *Metody ul'trazvukovoi defektoskopii* (Methods of Ultrasonic Flaw Detection), Leningrad: Mosk. Gorn. Inst., 1966.
32. Kramorov, G.A. and Evsyukov, V.N., On the ratio of areas of flat-bottomed and corner reflectors, *Defektoskopiya,* 1972, no. 4, pp. 138–140.
33. Perevalov, S.P. and Reichman, A.Z., Acoustic path of an inclined finder for a corner type reflector, *Defektoskopiya,* Part I, 1979, no. 11, pp. 5–15; Part 2, 1979, no. 12, pp. 28–36.
34. https://a3-eng.com/ultrazvukovoj-kontrol. Accessed January 22, 2024.
35. Golubev, A.S., Reflection of plane waves from a cylindrical defect, *Defektoskopiya,* 1961, no. 7, pp. 174–180.
36. Aleshin, N.P. and Mogil'ner, L.Yu., Analysis of the elastic field of ultrasonic waves scattered by a cylindrical cavity, *Defektoskopiya,* 1982, no. 12, pp. 18–29.
37. Mogil'ner, L.Yu., The use of a cylindrical reflector to adjust the sensitivity during ultrasonic testing, *Defektoskopiya,* 2018, no. 7, pp. 27–36.
38. Mogilner, L.Yu. and Smorodinskii, Ya.G., Ultrasonic flaw detection: Adjustment and calibration of equipment using samples with cylindrical drilling, *Russ. J. Nondestr. Test.,* 2018, no. 9, pp. 630–637.
39. *ASME T-530.* Ultrasonic testing of welded joints.
40. *ISO 18611.* Nondestructive testing—Ultrasonic testing—Sensitivity and range setting, 2014.
41. Ermolov, I.N., Vopilkin, A.Kh., and Badalyan, V.G., *Raschety v ul'trazvukovoi defektoskopiii (Kratkii spravochnik)* (Calculations in Ultrasonic Flaw Detection: A Brief Reference), Moscow: Ekho+, 2004.
42. Chernov, V.S., Quality control of welded joints of small diameter pipes: X-ray or ultrasound, *V Mire NK,* 2002, no. 2 (16), pp. 32–39.
43. The official server of Altes. http://ultes.info. Accessed March 15, 2024.
44. Aleshin, N.P., Baranov, V.Yu., Lezhava, A.G., and Mogil'ner, L.Yu., Setting the sensitivity of ultrasonic inspection by vertical cylindrical hole, *Defektoskopiya,* 1989, no. 10, pp. 23–29.
45. Aleshin, N.P., Lezhava, A.G., and Mogil'ner, L.Yu., The study of elastic wave diffraction by channel defects and recommendations for improving their detectability, *Defektoskopiya,* 1986, no. 11, pp. 4–10.
46. Silk, M.G., *Ultrasonic Transducers for Nondestructive Testing,* Bristol: Adam Hilger, 1984.
47. *ISO 10863.* Nondestructive testing of welds—Ultrasonic testing—Use of time-of-flight diffraction technique (TOFD), 2020.
48. Aleshin, N.P., Mogil'ner, L.Yu., Shchipakov, N.A., Kusii, A.G., Tishkin, V.V., and Degtyarev, M.N., On use of slots in modelling cracks in ultrasonic testing, *Russ. J. Nondestr. Test.,* 2022, vol. 58, no. 2, pp. 71–80.
49. Mel'nikova, A.V., Misharin, D.A., Bogdanov, R.I., and Ryakhovskikh, I.V., Substantiation of the operability of main gas pipelines with stress corrosion cracking defects, *Korroz. Territ. NEFTEGAZ,* 2015, no. 2 (31), pp. 32–40.
50. Aleshin, N.P., Krys'ko, N.V., Shchipakov, N.A., and Kusii, A.G., Ultrasonic control and complex application of flaw detection methods in the diagnosis of main pipelines, *Nauka Tekhnol. Truboprovodn. Transp. Nefti Nefteprod.,* 2023, no. 13 (1), pp. 8–17.
51. Kolesnikov, O.I., Geit, A.V., and Golosov, P.S., The limits of applicability of the diffraction-time control method at pipeline transport facilities, *Nauka Tekhnol. Truboprovodn. Transp. Nefti Nefteprod.,* 2022, no. 12 (6), pp. 560–568.

52. Mogil'ner, L.Yu., Kis'ko, N.V., Idrisov, M.T., and Kusii, A.G., The experience of using TOFD ultrasonic technology in the diagnosis of RVS, *Nauka Tekhnol. Truboprovodn. Transp. Nefti Nefteprod.,* 2023, no. 13 (5), pp. 411–421.
53. *RD 34.17.302-97 (OP 501 CD-97).* Steam and hot water boilers. Steam and hot water pipelines, vessels. Welded joints. Quality control. Ultrasonic monitoring. The main provisions, 1997.
54. Basatskaya, L.V., Voronkov, V.A., and Staseev, V.G., Measuring sensitivity with ultrasound control, *Tyazh. Mashinostr.,* 2000, no. 4, pp. 24–26.
55. Rozina, M.V., DAC diagrams. Where is the truth?, *V Mire NK,* 1999, no. 3, p. 28.
56. Danilov, V.N. and Voronkov, V.A., On the construction of DAC diagrams, *V Mire NK,* 2001, no. 2 (12), pp. 20–22.
57. Danilov, V.N. and Voronkov, V.A., Sensitivity calibration of ultrasonic detectors based using ADD diagrams, *Russ. J. Nondestr. Test.,* 2001, vol. 37, no. 1, pp. 44–47.
58. Mogil'ner, L.Yu. and Krys'ko, N.V., Scattering of ultrasonic waves by defects in welds and base material. Development of analytical and applied solutions, *Kontrol' Diagn.,* 2024, no. 3, pp. 4–13.
59. Samokrutov, A.A. and Shevaldykin, V.G., Ultrasonic tomography of metal structures using the digitally focused antenna array method, *Russ. J. Nondestr. Test.,* 2011, vol. 47, no. 1, pp. 21–28.
60. Samokrutov, A.A., Shevaldikin, V.G., and Smorodinskii, Ya.G., The terms of ultrasonic inspection with antenna arrays and what they mean, *Defektoskopiya,* 2018, no. 9, pp. 31–40.
61. Coulder, A., Full Matrix Capture and Total Focusing Method: The next evolution in ultrasonic testing, *Mater. Eval.,* 2018, no. 76 (5), pp. 591–597.
62. https://acsys.ru/vozmozhnosti-otsenki-kharactera-nesploshnosti-metallaultrazvukovym-tomografom. Accessed December 18, 2023.
63. Aleshin, N.P., Mogil'ner, L.Yu., Lisin, Y.V., Krys'ko, N.V., Pridein, O.A., and Idrisov, M.T., Features of crack detection during ultrasonic inspection of welded joints of the vertical steel tank wall, *Neft. Khoz.,* 2022, no. 1, pp. 86–91.
64. Boikov, A.V., Payor, V.A., Savel'ev, R.S., and Kolesnikov, A., Synthetic data generation for steel defect detection and classification using deep learning, *Symmetry,* 2021, no. 13, p. 1176. https://doi.org/10.3390/sym13071176
65. The Value of DICONDE. Koetz, Andrea and Clendening, Sue. s.l.: *NDT.net*, 2008.
66. Peloquin, E., The NDE 4.0 journey: How adopting a universal open format empowers the whole industry, *e-J. Nondestr. Test. (eJNDT Articles & News),* vol. 29 (1). https://blog.asnt.org/the-nde-4-0-journey-how-adopting-a-universal-open-format-empowers-the-wholeindustry. Accessed January 9, 2024.